

# Electromagnetic dissociation of ${}^8\text{B}$ and the astrophysical S factor for ${}^7\text{Be}(p, \gamma){}^8\text{B}$

B. Davids\*

*Kernfysisch Versneller Instituut, Zernikelaan 25, 9747 AA Groningen, The Netherlands*

S. Typel†

*Gesellschaft für Schwerionenforschung mbH, Planckstr. 1, 64291 Darmstadt, Germany*

(Dated: January 29, 2020)

We present S factor data obtained from the Coulomb dissociation of 83 MeV/nucleon  ${}^8\text{B}$ , and analyze  ${}^7\text{Be}$  longitudinal momentum distributions measured at 44 and 81 MeV/nucleon using a potential model, first-order perturbation theory, and dynamical solution of the time-dependent Schrödinger equation. Comparing our results with independent continuum-discretized coupled channels calculations, we examine the reaction model and beam energy dependence of the  $E2$  contribution to the dissociation cross section. By fitting radiative capture and Coulomb breakup data taken below relative energies of 400 keV with a potential model constrained by  ${}^7\text{Be} + p$  elastic scattering data, we examine the mutual consistency of recent  $S_{17}$  measurements. Evaluating the central values consistently and the extrapolation uncertainties on a case-by-case basis, we take a weighted average of the results of four direct and four indirect measurements to obtain a recommended value for  $S_{17}(0)$  of  $18.9 \pm 1.0$  eV b (95% confidence level).

PACS numbers: 25.70.De, 26.20.+f, 26.65.+t, 27.20.+n

With the discovery that a large fraction of the high-energy electron neutrinos emitted in the  $\beta^+$  decay of  ${}^8\text{B}$  in the sun are transformed into other active neutrino flavors on their way to terrestrial detectors [1], and, consistent with CPT symmetry, that reactor-produced antineutrinos also oscillate [2], a robust solution of solar neutrino problem seems to be in hand. Although the SNO neutral current measurement of the  ${}^8\text{B}$  solar neutrino flux is consistent with the predictions of the standard solar model [3], its precision is still far from that required to ascertain if there is transformation of solar electron neutrinos into sterile neutrinos [4, 5]. In order to reach this goal, the precision of both the experimental measurement and the theoretical prediction must be improved. Through the addition of NaCl and  ${}^3\text{He}$  proportional counters to the SNO detector, its neutral current measurement will be made much more precise. In order to improve the precision of the theoretical prediction of the  ${}^8\text{B}$  neutrino flux, the rate of the reaction that produces  ${}^8\text{B}$  in the sun,  ${}^7\text{Be}(p, \gamma){}^8\text{B}$ , must be better determined. Currently, the uncertainty on the zero-energy astrophysical S factor for this reaction,  $S_{17}(0)$  makes the largest contribution to the theoretical error budget.

Despite the profusion of recent determinations of  $S_{17}(0)$  [6, 7, 8, 9, 10, 11, 12, 13, 14, 15, 16, 17], the current recommendation [18] is based on the results of a single experimental measurement [19]. Recently, a weighted mean of such determinations based on both direct and indirect methods was given [20]. Here, we present data obtained via the indirect method of Coulomb dissociation [21], offer theoretical analyses of these and other data,

and assess the current state of knowledge of  $S_{17}(0)$ .

At solar energies, the radiative capture  ${}^7\text{Be}(p, \gamma){}^8\text{B}$  is entirely  $E1$  dominated. The Coulomb dissociation of  ${}^8\text{B}$  at intermediate beam energies also proceeds predominantly via  $E1$  transitions, but the much larger flux of  $E2$  virtual photons leads to a finite  $E2$  contribution to the dissociation cross section. This complicates efforts to extract the  $E1$  strength that determines the radiative capture rate. Since the first measurement of the Coulomb dissociation of  ${}^8\text{B}$  [22], the role of  $E2$  transitions in this process has been rather controversial. Experimental efforts to determine the  $E2$  contribution to the breakup cross section have focused on the relative energy and  ${}^8\text{B}$  scattering angle distributions [8, 23], the angular distributions [17] and longitudinal momentum distributions of the emitted protons [12], and the longitudinal momentum distributions of the  ${}^7\text{Be}$  fragments [24, 25]. The relative energy and  ${}^8\text{B}$  scattering angle distributions are relatively insensitive to  $E2$  strength, since the  $E1$  and  $E2$  contributions sum incoherently [26]. In contrast, the fragment longitudinal momentum and angular distributions are better suited to this task because interference between  $E1$  and  $E2$  transition amplitudes produces striking asymmetries in these distributions [27].

A first-order perturbation theory analysis of  ${}^7\text{Be}$  longitudinal momentum distributions found that the  $E2$  matrix elements implicit in the potential model used had to be scaled by  $0.7^{+0.3}_{-0.2}$  in order to best fit the measured distributions [20]. In that work, the idea that higher-order dynamical effects quench the  $E2$  strength predicted by first-order theories was advocated. Support for this idea was provided by concurrent [20] and subsequent [28] continuum-discretized coupled channels (CDCC) calculations. The perturbative calculations [27] employ a simple, single-particle model for the structure of  ${}^8\text{B}$ , and calculate the electromagnetic dissociation cross section

---

\*davids@kvi.nl

†s.typel@gsi.de

assuming single photon exchange, neglecting nuclear-induced breakup. The CDCC calculations use a similar structure model, but include electromagnetic and nuclear matrix elements to all orders. In Ref. [28], the authors found that a scaling of the  $E2$  matrix elements by a factor of 1.6 was required for the best description of the data. Hence the  $E2$  strength had to be reduced in first-order calculations, and enhanced in all-order calculations, relative to the original structure model predictions.

Here we study the same longitudinal momentum distributions [20] using two approaches, first-order perturbation theory and dynamical solution of the time-dependent Schrödinger equation [29]. Both methods employ only Coulomb matrix elements, and assume the same single-particle potential model. In this model, the p-wave potential depth has been fixed by the  $^8\text{B}$  binding energy, and the depths of the potentials for all other partial waves have been fixed by the s-wave scattering lengths for channel spin 1 and 2 in the  $^7\text{Be} + p$  system [30]. The potential radius is 2.5 fm, the diffuseness 0.65 fm, and the p-wave potential depth is 43.183 MeV. For s-, d-, and f-waves, the potential depths are 24.283 MeV and 51.898 MeV for  $S = 1$  and  $S = 2$  respectively. Spectroscopic factors for the two spin configurations were taken from Ref. [27] after a center-of-mass correction, and are 0.3231 for  $S = 1$  and 0.8572 for  $S = 2$ . Our potential model and that used in Ref. [28] differ from that of Ref. [27] in that they lack a spin-orbit interaction. As a result, our potential model predicts less  $E2$  strength near the  $M1$  resonance than does that of Ref. [27]. The model predicts  $S_{E2}/S_{E1}(0.6 \text{ MeV}) = 5.9 \times 10^{-4}$ . We have scaled the  $E2$  matrix elements calculated with our potential model, and then performed perturbative and dynamical calculations with the different  $E2$  scaling factors. After convoluting the calculations with the experimental momentum resolution of 5 MeV/c, and allowing the overall normalization to vary freely, we have determined the  $E2$  scaling factor that minimizes the  $\chi^2$  value for the central six 44 MeV/nucleon data points and the central five 81 MeV/nucleon data points of the measured longitudinal momentum distributions.

Fig. 1 shows the results of the best-fit calculations for the breakup of  $^8\text{B}$  on Pb at 44 MeV/nucleon, while Fig. 2 shows the 81 MeV/nucleon results. Both the perturbative and the dynamical calculations satisfactorily reproduce the measured asymmetries in the longitudinal momentum distributions. The required overall normalization factors range from 0.7 to 0.95 for the various angle cuts, beam energies, and reaction models. Consistent with earlier findings [20, 27, 28, 31], higher-order effects present in the dynamical calculations but neglected in the first-order perturbative calculations tend to reduce the asymmetry predicted for a given  $E2$  strength. Hence smaller  $E2$  scaling factors are required for the perturbative calculations than for the dynamical calculations. In addition, and quite unexpectedly, there is a hint of a beam energy dependence, with less  $E2$  strength required to explain the asymmetries observed at the higher beam

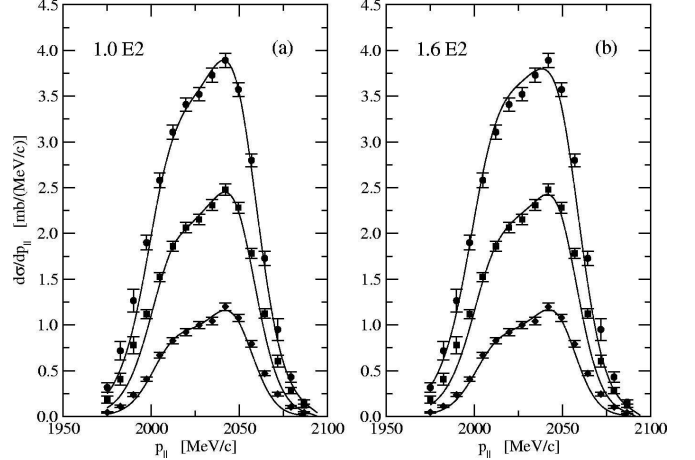


FIG. 1: Measured  $^7\text{Be}$  longitudinal momentum distributions from the Coulomb dissociation of 44 MeV/nucleon  $^8\text{B}$  on Pb with  $^7\text{Be}$  scattering angle cuts of  $1.5^\circ$ ,  $2.4^\circ$ , and  $3.5^\circ$ . Only relative errors are shown. The solid curves in panel (a) are the results of first-order perturbation theory calculations, while panel (b) shows dynamical calculations. In both cases the  $E2$  matrix elements have been scaled by the indicated factor.

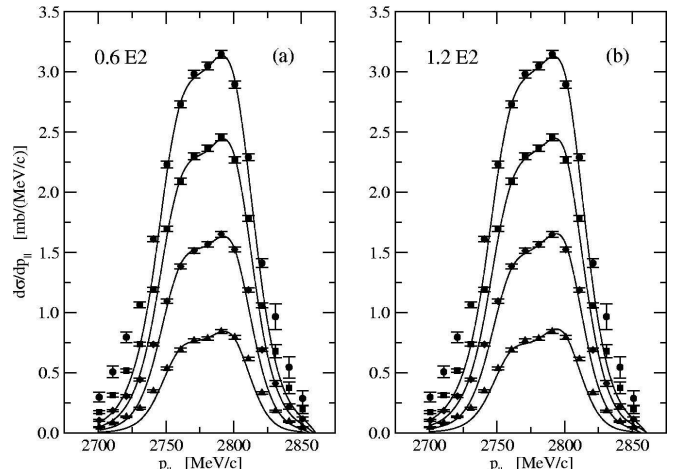


FIG. 2: Measured  $^7\text{Be}$  longitudinal momentum distributions from the Coulomb dissociation of 81 MeV/nucleon  $^8\text{B}$  on Pb with  $^7\text{Be}$  scattering angle cuts of  $1.0^\circ$ ,  $1.5^\circ$ ,  $2.0^\circ$ , and  $2.5^\circ$ . Only relative errors are shown. The solid curves in panel (a) are the results of first-order perturbation theory calculations, while panel (b) shows dynamical calculations. In both cases the  $E2$  matrix elements have been scaled by the indicated factor.

energy than at the lower. Such an effect, which has thus far eluded theoretical explanation, may be responsible for the reported lack of evidence for  $E2$  contributions to Coulomb breakup at 254 MeV/nucleon [8, 17].

The best-fit  $E2$  matrix element scaling factors and their  $1\sigma$  uncertainties obtained using the two reaction models are shown in Table I. It is of interest to compare the results found here with those reported in Ref. [20], which were deduced from a perturbative analysis of the

TABLE I: Best-fit scaling factors of  $E2$  matrix elements predicted by our potential model obtained from fitting the longitudinal momentum distributions of  ${}^7\text{Be}$  fragments from the Coulomb dissociation of  ${}^8\text{B}$  on Pb. The uncertainties are  $1\sigma$  values.

Beam Energy (MeV/nucleon)	Calculation	Scaling Factor
44	perturbative	$1.01 \pm 0.21$
44	dynamical	$1.6 \pm 0.2$
81	perturbative	$0.63 \pm 0.12$
81	dynamical	$1.2 \pm 0.2$

$3.5^\circ$  44 MeV/nucleon longitudinal momentum distribution. The best-fit scaling factor obtained from comparison of our perturbative calculation with the same data here implies  $S_{E2}/S_{E1}(0.6 \text{ MeV}) = 5.9_{-2.1}^{+2.6} \times 10^{-4}$ , which is consistent with the value of  $4.7_{-1.3}^{+2.0} \times 10^{-4}$  given in Ref. [20]. From this we conclude that the results of perturbative analyses favored thus far by workers in the field are relatively insensitive to the details of the underlying structure model. This analysis corroborates the case for including  $E2$  contributions in theoretical descriptions of the Coulomb breakup of  ${}^8\text{B}$  at beam energies below 100 MeV/nucleon.

One can also compare the results obtained here with dynamical calculations to those found using CDCC calculations in Ref. [28]. Those authors studied both the 44 MeV/nucleon and 81 MeV/nucleon longitudinal momentum distributions. Although no uncertainty was specified, the best-fit scaling value reported in Ref. [28] is 1.6, in perfect agreement with the value of  $1.6 \pm 0.2$  found from the dynamical analysis of 44 MeV/nucleon data here. Our result for the 81 MeV/nucleon data is somewhat smaller, but if the CDCC scaling factor uncertainty is comparable to that found here, the two results agree reasonably well at this beam energy also. Since the potential model assumed in the CDCC calculations is very similar to that employed here, we conclude that these two very different methods predict the same influence of higher-order effects. We therefore consider these predictions to be robust, and conclude that the practice of scaling the  $E2$  matrix elements in first-order perturbative calculations is a reasonable and practical way to proceed with the analysis of  ${}^8\text{B}$  Coulomb dissociation experiments.

In Ref. [12], an exclusive measurement of the Coulomb dissociation of 83 MeV/u  ${}^8\text{B}$  on a Pb target was described and experimental data were presented in graphical form, including the Coulomb dissociation cross section for  ${}^8\text{B}$  scattering angles  $\leq 1.77^\circ$ . This experimentally measured cross section was interpreted in the context of first-order perturbation theory in order to obtain  $S_{17}(0)$ . Here we give the energy-dependent S factor derived from these data in both graphical and tabular form. Table II contains the measured cross sections and their total  $1\sigma$  uncertainties. The systematic uncertainty common to each

TABLE II: Experimentally measured cross section for the Coulomb dissociation of 83 MeV/u  ${}^8\text{B}$  on Pb for  ${}^8\text{B}$  laboratory scattering angles of  $1.77^\circ$  and less (impact parameters  $\geq 30 \text{ fm}$ ), and astrophysical S factor for the  ${}^7\text{Be}(p, \gamma){}^8\text{B}$  reaction. The uncertainties are  $1\sigma$  values, and the systematic uncertainty common to each point is 7.1%.

$E_{rel}$ (MeV)	$d\sigma/dE_{rel}$ (mb/MeV)	$S_{17}(E_{rel})$ (eV b)
0.064	$9.0 \pm 2.8$	
0.192	$50.4 \pm 4.9$	$15.2 \pm 1.5$
0.384	$113.2 \pm 10.1$	$16.1 \pm 1.4$
0.768	$116.1 \pm 10.9$	$19.3 \pm 1.8$
1.280	$61.2 \pm 6.8$	$23.3 \pm 2.6$
1.792	$41.9 \pm 5.9$	$35.2 \pm 5.0$

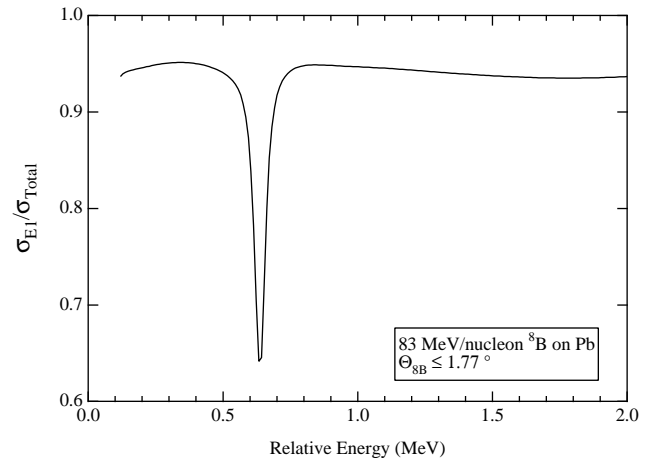


FIG. 3: Fraction of the calculated cross section for the Coulomb dissociation of 83 MeV/nucleon  ${}^8\text{B}$  on Pb with  ${}^8\text{B}$  scattering angles  $\leq 1.77^\circ$  ( $b \geq 30 \text{ fm}$ ) accounted for by  $E1$  transitions in first-order perturbation theory. As the energy falls below 100 keV,  $E2$  transitions become increasingly important. The dip is due to the 630 keV  $M1$  resonance.

point amounts to 7.1%, and includes contributions from the target thickness (1%), beam intensity (2.6%), momentum calibration (4.2%), and the size of the  $E2$  component (5%).

The fraction of the measured cross section accounted for by  $E1$  transitions in first-order perturbation theory using the potential model of Esbensen and Bertsch [27] is shown in Fig. 3. Recent calculations found that this  $E1$  fraction is nearly model independent at low relative energies [32]. Astrophysical S factors derived from the experimental cross section data are shown in Fig. 4, Fig. 5, and Table II. These S factors have been corrected for the  $E2$  contribution to the breakup cross section in the following way. The measured cross section was multiplied by the  $E1$  fraction shown in Fig. 3 to obtain the  $E1$  cross section, from which the S factor was deduced using semiclassical first-order Coulomb excitation theory [33], taking into account the experimental relative energy

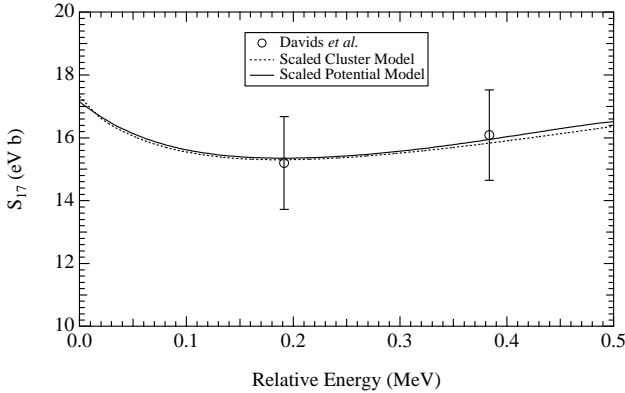


FIG. 4: Astrophysical S factor for the  ${}^7\text{Be}(p, \gamma){}^8\text{B}$  reaction at low relative energies measured via the Coulomb dissociation of 83 MeV/u  ${}^8\text{B}$  on Pb. The systematic uncertainty common to each point is 7.1%. The solid curve is our potential model calculation, which has been scaled by a factor 0.62, and the dashed curve is the Descouvemont and Baye cluster model scaled by 0.57. The two calculations agree very well below 400 keV.

resolution. Owing to uncertainty regarding the size of higher-order dynamical effects at very low relative energies [34], we have not extracted an S factor for the lowest energy data point. In order to minimize the uncertainties due to nuclear structure in extrapolating the astrophysical S factor to zero energy, it has been recommended that only data obtained below 400 keV be considered [35]. This low energy regime is shown in Fig. 4. Two theoretical calculations are also shown in the figure, representing the best fits using our potential model and the Descouvemont and Baye cluster model [36] that assumed the Volkov II force. The former was scaled by 0.62, while the latter was multiplied by 0.57. The shapes of the two models agree very well below 400 keV, and the extrapolated zero-energy S factors using the two data points in that energy range differ by only 0.6%. Using the potential model to fit these low energy data yields a value of  $S_{17}(0) = 17.2 \pm 1.1$  eV b, where the  $1\sigma$  uncertainty is purely experimental.

Although our potential model and the cluster model of Ref. [36] agree very well at low energies, other choices of potential model parameters lead to different results. This is illustrated in Fig. 5, where two potential model calculations are shown along with the 83 MeV/nucleon Coulomb breakup S factor data. The solid line is the potential model described above and shown in Fig. 4, while the dashed curve represents a potential model calculation with the same spectroscopic factors but with the s-, d-, and f-wave potential depths adjusted to reproduce the scattering lengths measured in the isospin mirror  ${}^7\text{Li} + n$  system [37]. The potential depths in this case are 43.857 MeV and 52.597 MeV for  $S = 1$  and  $S = 2$  respectively. Both calculations have been scaled to optimally fit the data points below 400 keV, and both reproduce the data well. However, the extrapolated values differ by more

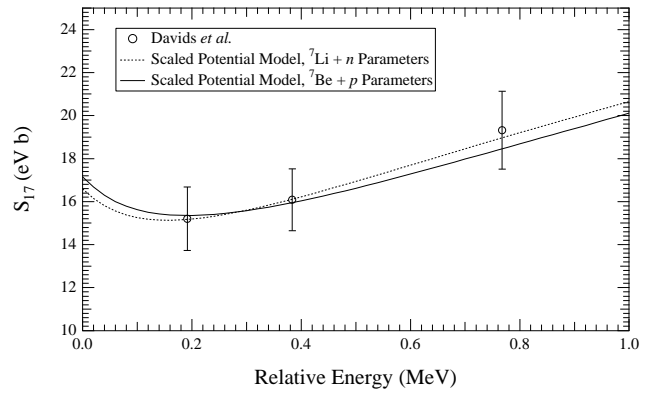


FIG. 5: Astrophysical S factor for the  ${}^7\text{Be}(p, \gamma){}^8\text{B}$  reaction obtained from the Coulomb dissociation of 83 MeV/u  ${}^8\text{B}$  on Pb. Potential-model calculations using parameters fixed by  ${}^7\text{Be} + p$  and  ${}^7\text{Li} + n$  elastic scattering data are also shown. The calculations have been scaled to best fit the data below 400 keV, and the difference between their values at zero energy is taken as the extrapolation uncertainty of this measurement.

than 3%. This fact exposes the danger of using high relative energy data (above the  $M1$  resonance) to extrapolate to zero energy. Here, even limiting the relative energy range to  $< 400$  keV and considering only models that reproduce the available elastic scattering data, the extrapolation uncertainty is appreciable. Although the scattering lengths have been measured for the  ${}^7\text{Be} + p$  system, they are not as precisely measured as those for the mirror  ${}^7\text{Li} + n$  system. The measured  ${}^7\text{Be} + p$  and  ${}^7\text{Li} + n$  scattering lengths for the dominant  $S = 2$  channel are consistent with isospin symmetry, but there is an inconsistency for the  $S = 1$  channel that requires further study. We therefore use the potential-model parameters fixed by  ${}^7\text{Be} + p$  elastic scattering data [30], but regard the difference between the extrapolated values using the two potential-model parameter sets as the extrapolation uncertainty. Adding this extrapolation error in quadrature with the experimental uncertainties, we obtain  $S_{17}(0) = 17.2 \pm 1.3$  eV b.

We fit the data of Filippone *et al.* [19], Hammache *et al.* [13], Strieder *et al.* [9], Junghans *et al.* [15], Baby *et al.* [16], and Schümann *et al.* [17] using the same procedure. The results of this extrapolation of data below relative energies of 400 keV using our potential model are shown in Table III. The Filippone *et al.* data have been renormalized using the weighted average of their two target thickness measurements after adjusting that based on the  ${}^7\text{Li}(d, p){}^8\text{Li}$  reaction using the cross section recommended in [18]. They have not been corrected for  ${}^8\text{B}$  backscattering losses. Considering only experimental uncertainties, a weighted average of all these measurements gives a  $\chi^2$  of 37.9 for six degrees of freedom, which indicates inconsistency. Excluding the measurement of Junghans *et al.*, we find a  $\chi^2$  of 5.1 for five degrees of freedom, showing that the other six measurements are consistent.

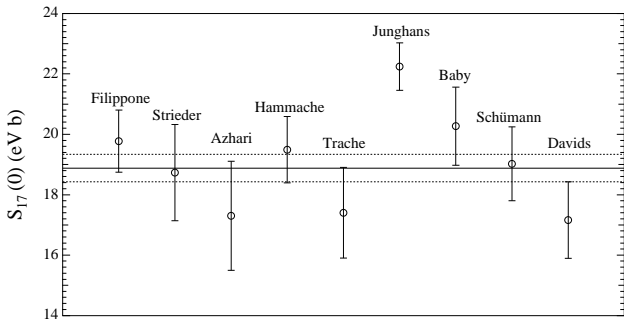


FIG. 6: Zero energy astrophysical S factors for the  ${}^7\text{Be}(p, \gamma){}^8\text{B}$  reaction based on experimental measurements at relative energies  $< 400$  keV extrapolated with a potential model constrained by  ${}^7\text{Be} + p$  elastic scattering data. The  $1\sigma$  total uncertainties include extrapolation contributions evaluated individually for each measurement as explained in the text. Also shown are the ANC results of Azhari *et al.* and Trache *et al.* A weighted mean of eight of these nine measurements yields  $18.9 \pm 0.5$  eV b ( $1\sigma$ ), with  $\chi^2 = 5.8$  for seven degrees of freedom. This weighted average and its 68% confidence level band are also depicted.

Individual experimental results were obtained by fitting the data below 400 keV with our potential model, which is constrained by  ${}^7\text{Be} + p$  elastic scattering data. Extrapolation uncertainties were determined on a case-by-case basis by taking the difference between these results and those obtained using the potential model fit to  ${}^7\text{Li} + n$  elastic scattering data, which are always smaller than the values extrapolated with the  ${}^7\text{Be} + p$  potential model parameters. We add the experimental and extrapolation uncertainties in quadrature to obtain the total uncertainties given in Table III.

Zero energy astrophysical S factors for the  ${}^7\text{Be}(p, \gamma){}^8\text{B}$  reaction based on experimental measurements at relative energies  $< 400$  keV extrapolated with our potential model are shown in Fig. 6. Also shown are the values

of  $S_{17}(0)$  determined from asymptotic normalization coefficients (ANCs) by Azhari *et al.* [11],  $17.3 \pm 1.8$  eV b, and Trache *et al.* [14],  $17.4 \pm 1.5$  eV b. A weighted mean of the six mutually consistent radiative capture and Coulomb breakup measurements plus the two ANC results yields  $18.9 \pm 0.5$  eV b ( $1\sigma$ ), with  $\chi^2 = 5.8$  for seven degrees of freedom. If this value were adopted, then the rate of the  ${}^7\text{Be}(p, \gamma){}^8\text{B}$  reaction would no longer be the largest theoretical uncertainty in the  ${}^8\text{B}$  solar neutrino flux. Rather, the radiative opacity and heavy element abundance of the sun and the  ${}^3\text{He}(\alpha, \gamma){}^7\text{Be}$  S factor would make larger contributions to the uncertainty in the theoretical  ${}^8\text{B}$  solar neutrino flux [38].

In summary, we have examined the reaction model and beam energy dependence of the  $E2$  contribution to the Coulomb dissociation of  ${}^8\text{B}$  through the comparison of  ${}^7\text{Be}$  longitudinal momentum distribution data with first-order perturbation theory, continuum-discretized coupled channels, and dynamical calculations. A coherent picture emerges when one considers seven precise direct and indirect measurements of the astrophysical S factor for the  ${}^7\text{Be}(p, \gamma){}^8\text{B}$  reaction, though one recent measurement is discrepant with the others. Evaluating the central values consistently and the extrapolation uncertainties on a case-by-case basis, we take a weighted average of the results of four direct and four indirect measurements to obtain a recommended value for  $S_{17}(0)$  of  $18.9 \pm 1.0$  eV b (95% confidence level), with  $\chi^2 = 5.8$  for seven degrees of freedom. If this value were adopted in solar models, the  ${}^7\text{Be}(p, \gamma){}^8\text{B}$  reaction rate would no longer represent the dominant uncertainty in the theoretical prediction of the high-energy solar neutrino flux.

### Acknowledgments

BD acknowledges fruitful discussions with Sam Austin, Carlos Bertulani, Henning Esbensen, Christian Forssén, Byron Jennings, and Livius Trache.

---

[1] Q. R. Ahmad, R. C. Allen, T. C. Andersen, J. D. Anglin, J. C. Barton, E. W. Beier, M. Bercovitch, J. Bigu, S. D. Biller, R. A. Black, *et al.*, *Phys. Rev. Lett.* **89**, 11301 (2002).

[2] K. Eguchi, S. Enomoto, K. Furuno, J. Goldman, H. Hanada, H. Ikeda, K. Ikeda, K. Inoue, K. Ishihara, W. Itoh, *et al.*, *Phys. Rev. Lett.* **90**, 21802 (2003).

[3] J. N. Bahcall, M. H. Pinsonneault, and S. Basu, *Astrophys. J.* **555**, 990 (2001).

[4] V. Barger, D. Marfatia, K. Whisnant, and B. P. Wood, *Phys. Lett. B* **537**, 179 (2002).

[5] J. N. Bahcall, M. C. Gonzalez-Garcia, and C. Peña-Garay, *Phys. Rev. C* **66**, 35802 (2002).

[6] T. Kikuchi, T. Motobayashi, N. Iwasa, Y. Ando, M. Kurokawa, S. Moriya, H. Murakami, T. Nishio, J. Ruan, S. Shirato, *et al.*, *Eur. Phys. J. A* **3**, 213 (1998).

[7] M. Hass, C. Broude, V. Fedoseev, G. Goldring, G. Huber, J. Lettry, V. Mishin, H. J. Ravn, V. Sebastian, and L. Weissman, *Phys. Lett. B* **462**, 237 (1999).

[8] N. Iwasa, F. Boué, G. Surówka, K. Sümmerer, T. Baumann, B. Blank, S. Czajkowski, A. Förster, M. Gai, H. Geissel, *et al.*, *Phys. Rev. Lett.* **83**, 2910 (1999).

[9] F. Strieder, L. Gialanella, G. Gyürky, F. Schümann, R. Bonetti, C. Broggini, L. Campajola, P. Corvisiero, H. Costantini, A. D'Onofrio, *et al.*, *Nucl. Phys. A* **696**, 219 (2001).

[10] F. Terrasi, L. Gialanella, G. Imbriani, F. Strieder, L. Campajola, A. D'Onofrio, U. Greife, G. Gyürky, C. Lubritto, A. Ordine, *et al.*, *Nucl. Phys. A* **688**, 539 (2001).

[11] A. Azhari, V. Burjan, F. Carstoiu, C. A. Gagliardi, V. Kroha, A. M. Mukhamedzhanov, F. M. Nunes,

TABLE III: Zero energy astrophysical S factors for the  ${}^7\text{Be}(p, \gamma){}^8\text{B}$  reaction obtained by extrapolating radiative capture and Coulomb dissociation data at  $E_{\text{rel}} < 400$  keV with a potential model constrained by  ${}^7\text{Be} + p$  elastic scattering data. Extrapolation uncertainties are evaluated as described in the text. All uncertainties are  $1\sigma$  values.

First Author	Reference	$S_{17}(0)$ (eV b)	Experimental Error (eV b)	Extrapolation Error (eV b)	Total Error (eV b)
Filippone	[19]	19.8	0.8	0.7	1.0
Strieder	[9]	18.7	1.4	0.7	1.6
Hammache	[13]	19.5	0.9	0.7	1.1
Jungmans	[15]	22.2	0.3	0.7	0.8
Baby	[16]	20.3	1.0	0.8	1.3
Schümann	[17]	19.0	1.1	0.6	1.2
Davids	this work	17.2	1.1	0.6	1.3

X. Tang, L. Trache, and R. E. Tribble, Phys. Rev. C **63**, 55803 (2001).

[12] B. Davids, D. W. Anthony, T. Aumann, S. M. Austin, T. Baumann, D. Bazin, R. R. Clement, C. N. Davids, H. Esbensen, P. A. Lofy, et al., Phys. Rev. Lett. **86**, 2750 (2001).

[13] F. Hammache, G. Bogaert, P. Aguer, C. Angulo, S. Barhoumi, L. Brillard, J. F. Chemin, G. Claverie, A. Coc, M. Hussonnois, et al., Phys. Rev. Lett. **86**, 3985 (2001).

[14] L. Trache, F. Carstoiu, C. A. Gagliardi, and R. E. Tribble, Phys. Rev. Lett. **87**, 271102 (2001).

[15] A. R. Junghans, E. C. Mohrman, K. A. Snover, T. D. Steiger, E. G. Adelberger, J. M. Casandjian, H. E. Swanson, L. Buchmann, S. H. Park, and A. Zyuzin, Phys. Rev. Lett. **88**, 41101 (2002).

[16] L. T. Baby, C. Bordeanu, G. Goldring, M. Hass, L. Weissman, V. N. Fedoseyev, U. Köster, Y. Nir-El, G. Haquin, H. W. Gäggeler, et al., Phys. Rev. Lett. **90**, 22501 (2003).

[17] F. Schümann, F. Hammache, S. Typel, F. Uhlig, K. Sümmeler, et al., nucl-ex/0304011 (2003).

[18] E. G. Adelberger, S. M. Austin, J. N. Bahcall, A. B. Balantekin, G. Bogaert, L. S. Brown, L. Buchmann, F. E. Cecil, A. E. Champagne, L. de Braeckeleer, et al., Rev. Mod. Phys. **70**, 1265 (1998).

[19] B. W. Filippone, A. J. Elwyn, C. N. Davids, and D. D. Koetke, Phys. Rev. C **28**, 2222 (1983).

[20] B. Davids, S. M. Austin, D. Bazin, H. Esbensen, B. M. Sherrill, I. J. Thompson, and J. A. Tostevin, Phys. Rev. C **63**, 65806 (2001).

[21] G. Baur, C. A. Bertulani, and H. Rebel, Nucl. Phys. A **458**, 188 (1986).

[22] T. Motobayashi, N. Iwasa, Y. Ando, M. Kurokawa, H. Murakami, J. Ruan (Gen), S. Shimoura, S. Shirato, N. Inabe, M. Ishihara, et al., Phys. Rev. Lett. **73**, 2680 (1994).

[23] T. Kikuchi, T. Motobayashi, N. Iwasa, Y. Ando, M. Kurokawa, S. Moriya, H. Murakami, T. Nishio, J. Ruan (Gen), S. Shirato, et al., Phys. Lett. B **391**, 261 (1997).

[24] J. H. Kelley, S. M. Austin, A. Azhari, D. Bazin, J. A. Brown, H. Esbensen, M. Fauerbach, M. Hellström, S. E. Hirzebruch, R. A. Kryger, et al., Phys. Rev. Lett. **77**, 5020 (1996).

[25] B. Davids, D. W. Anthony, S. M. Austin, D. Bazin, B. Blank, J. A. Caggiano, M. Chartier, H. Esbensen, P. Hui, C. F. Powell, et al., Phys. Rev. Lett. **81**, 2209 (1998).

[26] C. A. Bertulani and P. Danielewicz, Nucl. Phys. A **717**, 199 (2003).

[27] H. Esbensen and G. F. Bertsch, Nucl. Phys. A **600**, 37 (1996).

[28] J. Mortimer, I. J. Thompson, and J. A. Tostevin, Phys. Rev. C **65**, 64619 (2002).

[29] S. Typel and H. H. Wolter, Z. Naturforsch. **54a**, 63 (1999).

[30] C. Angulo, M. Azzouz, P. Descouvemont, G. Tabacaru, D. Baye, M. Cognéau, M. Couder, T. Davinson, A. di Pietro, P. Figuera, et al., Nucl. Phys. A **716**, 211 (2003).

[31] H. Esbensen and G. F. Bertsch, Phys. Rev. C **66**, 44609 (2002).

[32] C. Forssén, N. B. Shul'gina, and M. V. Zhukov, Phys. Rev. C (2003).

[33] K. Alder, A. Bohr, T. Huus, B. Mottelson, and A. Winther, Rev. Mod. Phys. **28**, 432 (1956).

[34] E. O. Alt, B. F. Irgaziev, and A. M. Mukhamedzhanov, Phys. Rev. Lett. **90**, 122701 (2003).

[35] B. K. Jennings, S. Karatagliidis, and T. D. Shoppa, Phys. Rev. C **58**, 3711 (1998).

[36] P. Descouvemont and D. Baye, Nucl. Phys. A **567** (1994).

[37] L. Koester, K. Knopf, and W. Waschkowski, Z. Phys. A **312**, 81 (1983).

[38] J. N. Bahcall, FORTRAN code Exportrates (2002).